

DOPPLER SPECTRUM TYPE CONTRIBUTION TO BER IN FIBER OPTIC COMMUNICATION CHANNEL

I. Vujović^{1*} – J. Šoda¹ – I. Kuzmanić¹

¹Department of Marine Electrical Engineering and Information Technologies, Faculty of Maritime Studies, University of Split, Zrinjsko-Frankopanska 38, Split, Croatia

ARTICLE INFO

Article history:

Received: 24.03.2015.

Received in revised form: 27.07.2015.

Accepted: 31.07.2015.

Keywords:

Noise

Communication channel

Fiber optic communication

Abstract:

Integrated ship communication systems require reliable and safe communication media that is suitable for fiber optic cables. This paper investigates such systems. The focus of this paper is on the research into the influences of different Doppler spectrum types to measure bit error rate in communications based on fiber optics. The results show that the highest BER is obtained for Asymmetrical Jakes and the lowest for the Jakes spectrum type. Although we are interested in communications aboard ships, the methodology can be applied to any fiber optic communication system.

1 Introduction

Fiber optic communication media is popular applications to computer and integrated networks, fiber optic local area networks (FOLANs), and the Internet. These networks are present both offshore and land applications.

Although ships appear relatively small in length, the actual length of all cables aboard is huge. Investigation of appropriate spectrum type leads to conclusions about appropriate type for desired bit error rate (BER).

There are several reasons for optical technology usage aboard vessels [1]:

- high reliability, no need for grounding, no worries about short circuits, overvoltage, fire, and similar;
- reduction of volume and weight up to 90% in comparison to copper wires;
- simple self-diagnostics;
- integration of all ship systems and subsystems by FOLAN;
- support of increase in capacity;

- long lifetime;
- resistivity to EM (Electro-Magnetic) disturbances and interferences;
- cheap and simple installation, and
- maintenance cost reduction.

Fiber optic media became an optimal media for application in dangerous, explosive and high temperature environments existing in the ships. Although we are primarily interested in ship communications, the paper can be applied to land and ship communications.

This is, however, not the first study of nonlinearities. So, the influence of the nonlinear effects was studied in [2]. A detailed analysis of all parts of the optic communication system is presented in [3]. A simulation platform for photonic transmission systems is presented in [4]. Cutting edge trends in fiber optic communication systems can be found i.e., in [4–7]. It can be seen that efforts are made in the direction of the development of high capacity super channels.

The paper is organized as follows. A fiber optic communication system model is presented in the

* Corresponding author. Tel.:38521380762; fax: 38521380759
E-mail address: ivujovic@pfst.hr.

second section. Simulation parameters and results are presented in the third section (for various spectrum types, namely Jakes, Bell, Flat, Gauss, Bi-Gauss, Rounded and Asymmetrical Jakes). A comparison of these spectrum types is also presented in this section. The last section gives the conclusions.

2 Simulation settings

2.1 Simulated system

Each communication system consists of the transmitter, the receiver part, and the communication channel. As the communication channel introduces errors into a communication process, it is, thus, the scope of this research paper. In the case of fiber optic media, the communication channel consists of the optical media (dielectric material). The transmitter part consists of:

- the signal source,
- the modulation block,
- the transmit filter, and
- the optic transmitter.

Transmission is modeled with the transmit filter.

Fiber optic media model must contain any shifts and changes which could be found in operation of the communication system. To simulate all influences, we used AWGN (Additive White Gaussian Noise) and Rayleigh fading. Finally, the receiver part consists of the optic receiver and demodulator. This is schematically shown in Fig. 1.

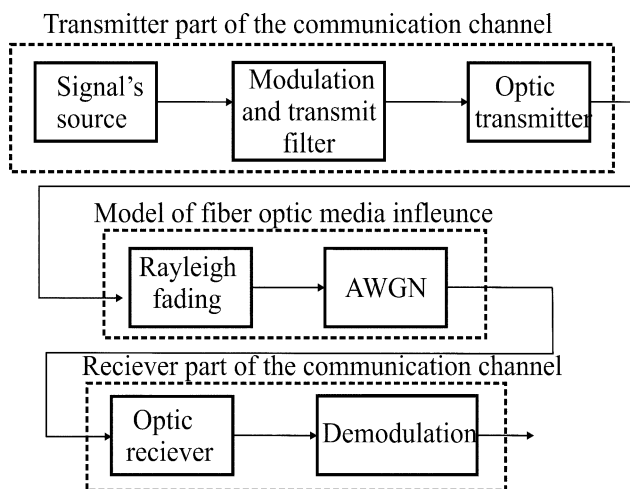


Figure 1. Fiber optic communication system model.

For the model in Fig. 1, Simulink simulation model has been developed. The simulation model is used for the experiments (simulations). Results are exported to Matlab and saved for an off-line analysis.

2.2 Additional information

Simulations were performed on Windows operating system in the Matlab/Simulink environment and the Communication System Toolbox. Only standard components were used for every part of the system in Fig. 1. Properties are further explained in the following section. A link between photonics and development of Simulink models for optic communications is given in [4]. A complete Simulink model for OFDM (Orthogonal frequency division multiplex) system is given in [8]. AWGN and Rayleigh fading is used in the model for the communication channel modeling. In [9], it is proven that Simulink is efficient for simulation of the fiber optic communications with minimum development and computational time. These references propose models for the fiber optic communication channel simulation in the Simulink environment.

Multipath has already been incorporated into Simulink blocks. However, Multipath is not superfluous. Multipath presents an extra safety property/level necessary for the critical information to reach the designated receiver. This information can be vital in the ship systems status monitoring and the prevention of the avalanche failure. Multipath is also safety redundancy management in case some naval progression paths are stopped due to damages in combat. It enables partially damaged communication system to operate, and satisfy its duty in the integration of the ship systems. Multipath can cause problems due to interference of different paths (see [10]).

Rayleigh fading and AWGN impact on optical communication systems can be further explored (see i.e. [11]). This signal is assumed to be a real-valued signal, $s_i(t)$, of duration T , which is described with energy:

$$E_i = \int_0^T s_i^2(t) dt. \quad (1)$$

It propagates over the optical channel with characteristics that the channel noise is a zero-mean

AWGN. AWGN originates from amplified spontaneous emission (ASE) noise due to optical amplifiers deployed on the line [11].

The Doppler shift (or the Doppler Effect) can be caused by mixing different modes or different paths, which can all be a separate study. However, it is not caused by usual reasons, such as movement of the observer, transmitter or receiver. Doppler shift can also be caused by scattered light in the optic material.

Frequency of the Doppler-shifted scattered light is:

$$f_s = f_p - f_b, \quad (2)$$

where f_p denotes that „pump“ is incident on a material medium, f_b denotes the medium of thermally-generated phonon, and f_s denotes scattered light frequency.

Not all phonons have exactly the same frequency. Lifetime broadening of the phonon line means that phonon frequency is in the approximate range of:

$$f_B = f_{B0} \pm \frac{\Delta f_B}{2}, \quad (3)$$

with $f_{B0} = \frac{nf_s}{\pi\lambda_0}$ and $\Delta f_B = \frac{1}{\pi\tau_{ph}}$ where n is the

refractive index of the medium, f_s is the velocity of sound, λ_0 is the optical wavelength, and τ_{ph} is the lifetime of a phonon.

Calculations show that this effect remains confined to a single channel of the optic communication link for infrared windows.

It would be also interesting for some readers to grasp the length of fiber optics aboard ships. It depends on the type and size of the ship. A cargo ship with fiber optic temperature sensors can have multiple ship length of optic fibers only for these sensors [12], without taking into account communication systems, ship’s LAN, integrated ship’s functions, etc.

Additional information about multipath in optical communication systems could also be found in [13], and for design of the optic communication system using Simulink, in [14]. Lasers (possible sources) were reviewed in [15].

3 Results and discussion

Our intention was to simulate the influence of the changes in fiber optic media on the transmitted

signal. Hence, it was interesting to simulate changes in the optic media parameters and examine the influence of these changes on the receiver part of the communication system. Therefore, parameters of the “media” were changing and the output constellation is observed. The ultimate goal should be to determine which spectrum type is the best in view of BER.

A subsystem is constructed in order to simulate the fiber optic channel. The subsystem consists of two blocks without I/O (see Fig. 2). Spectrum types and parameters for different spectrum types are adjusted in the Simulink block “Multipath Rayleigh Fading” (red circle in Fig. 2). Fig. 2 shows only a subsystem under mask, not the actual signals in the overall system.

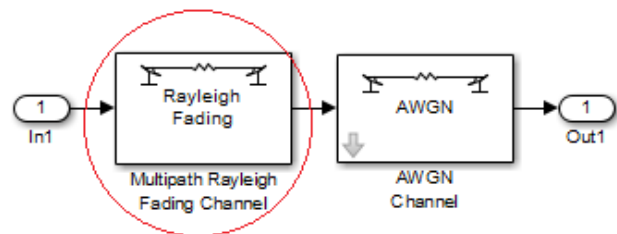


Figure 2. Fiber optic media – a subsystem (under the mask) within the simulation model.

Since there are different possibilities in modeling the optic fiber channel, all available spectrum types have been simulated. Setups for different spectrum types are as follows.

For the Asymmetrical Jakes spectrum type, setups are (Matlab denotation):

- Maximum Doppler shift (Hz): 100,
- Minimum and maximum Doppler frequencies, normalized by maximum Doppler shift: [0 1];
- Discrete path delay vector (s): [0 2e-6];
- Average path gain vector (dB): [0 -3];
- Initial seed: 73.

For the Bell spectrum type, setups are:

- Maximum Doppler shift 100 Hz;
- Bell coefficient 9;
- Discrete path delay vector [0 2e-6] s;
- Average path gain vector [0 -3] dB;
- Initial seed: 73.

For the Bi-Gaussian spectrum type, setups are:

- Maximum Doppler shift 100 Hz;
- Standard deviation of the 1st Gaussian function normalized by maximum Doppler

shift: $\frac{1}{\sqrt{2}}$;

- Standard deviation of the 2nd Gaussian function normalized by maximum Doppler shift: $\frac{1}{\sqrt{2}}$;
- Center frequency of 1st Gaussian function, normalized by maximum Doppler shift: 0.0;
- Center frequency of 2nd Gaussian function, normalized by maximum Doppler shift: 0.0;
- Power gain of 1st Gaussian function (linear scale): 0.5;
- Power gain of 2nd Gaussian function (linear scale): 0.5;
- Discrete path delay vector (s): [0 2e-6];
- Average path gain vector (dB): [0 -3];
- Initial seed: 73.

For the Rounded spectrum type, parameters used are:

- Maximum Doppler shift (Hz): 100;
- Polynomial coefficients of the Doppler spectrum: [1 - 1.72 0.785];
- Discrete path delay vector (s): [0 2e-6];
- Average path gain vector (dB): [0 - 3];
- Initial seed: 73.

For the Gaussian spectrum type, parameters are:

- Maximum Doppler shift (Hz): 100;
- Standard deviation of Gaussian function, normalized by maximum Doppler shift: $\frac{1}{\sqrt{2}}$;
- Discrete path delay vector (s): [0 2e-6];
- Average path gain vector (dB): [0 - 3];
- Initial seed: 73.

For the Flat spectrum type, parameters are:

- Maximum Doppler shift: 100 Hz;
- Discrete path delay vector (s): [0 2e-6];
- Average path gain vector (dB): [0 - 3];
- Initial seed: 73.

For the Jakes spectrum type, parameters are:

- Doppler 100 Hz;
- Discrete path delay vector (s): [0 2e-6];
- Average path gain vector (dB): [0 - 3];
- Initial seed: 73.

Fig. 3 shows BER in simulated time interval for all Doppler spectrum types for the same SNR (Signal-to-Noise Ratio). Fig. 3 shows that the waveform of BER over time has been similar for various spectrum types. This can mean that BER is not dependent on the spectrum type.

Table 1. presents results for the average BER in cases of all considered spectrum types at the same SNR.

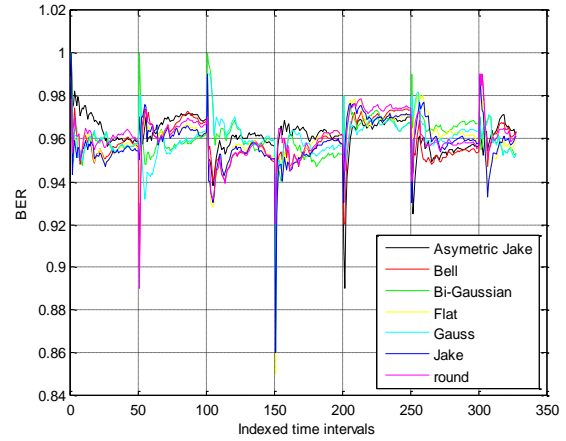
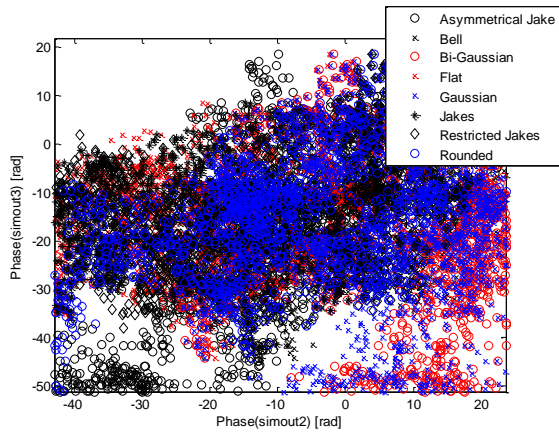


Figure 3. BER for change of Doppler spectrum type in Multipath Fading Channel Simulink block.

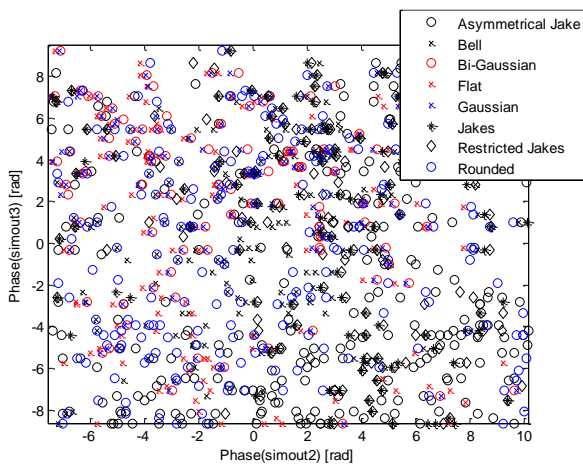
Table 1. Mean BER for different Doppler spectrum type – simulation results for the same SNR

Doppler spectrum type	BER
Jakes	0.9589
Bell	0.9595
Flat	0.9599
Gauss	0.9600
Bi-Gaussian	0.9607
Rounded	0.9610
Asymmetrical Jakes	0.9624

Following results show the influence of the SNR exerted on output constellation. Fig. 4 shows phases of end-to-end constellation, i.e., the phase of input-output relationship.



a)



b)

Figure 4. Phases of end-to-end constellation for various spectral types: a) lower zoom, b) higher zoom.

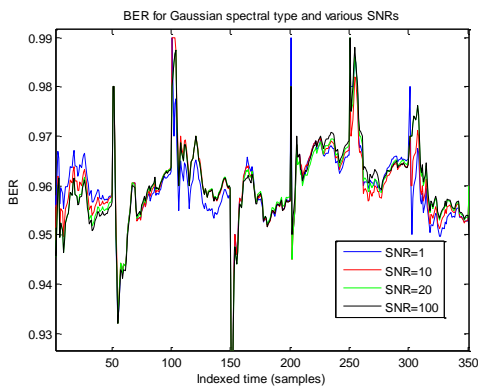


Figure 5. Time dependence of the SNR influence to the BER for the Gaussian spectral type (an enlarged part of the graph).

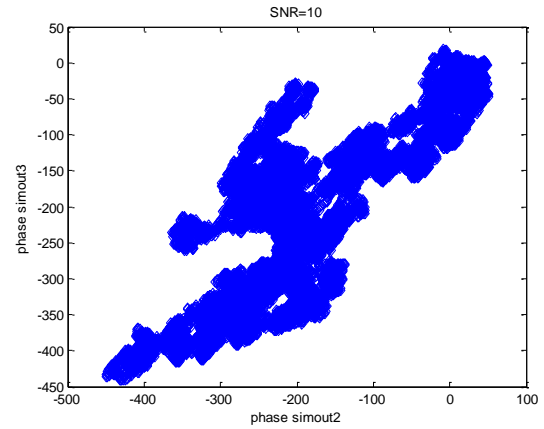


Figure 6. Phase of end-to-end constellation for SNR = 10 dB.

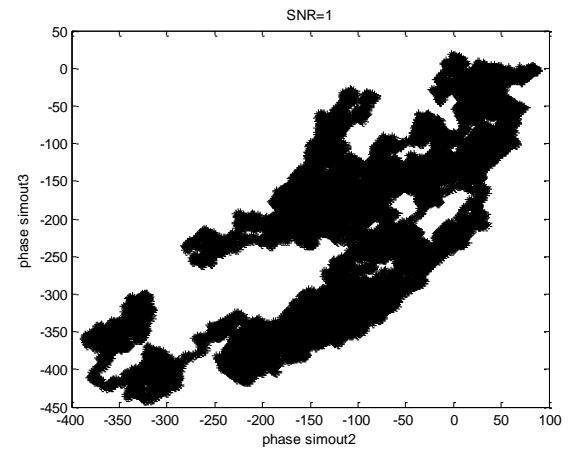


Figure 7. Phase of end-to-end constellation for SNR = 1 dB.

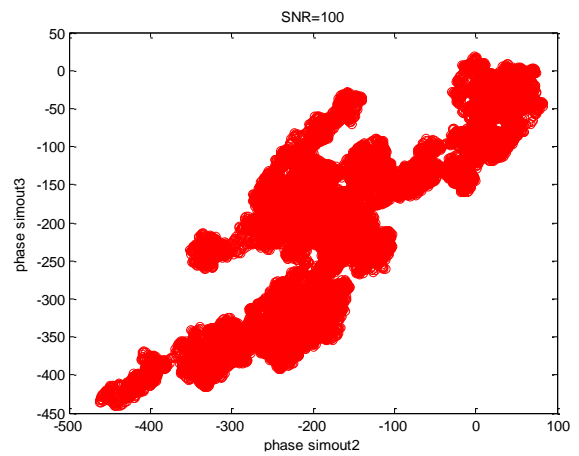


Figure 8. Phase of end-to-end constellation for SNR = 100 dB.

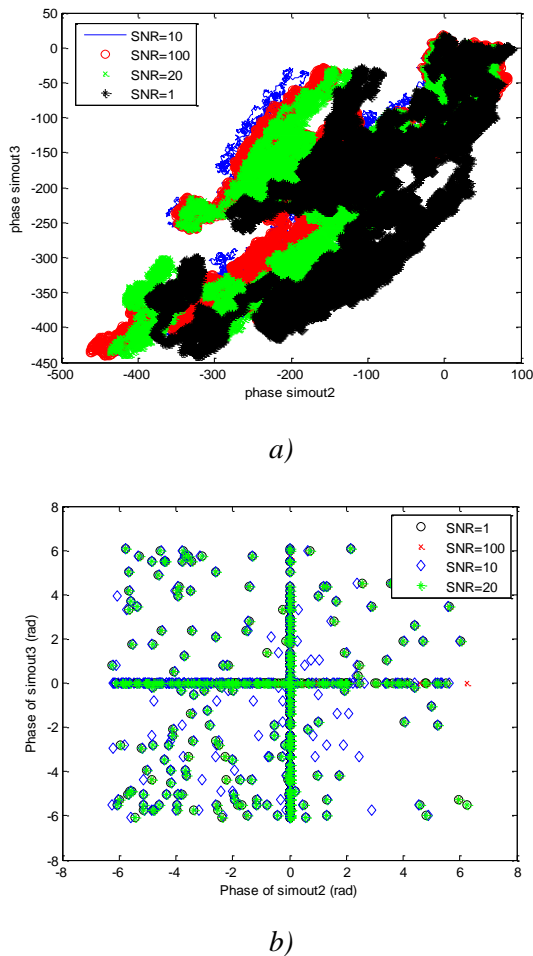


Figure 9. a) Comparison of the phase of the end-to-end constellation for SNRs 1, 10, 20, and 100 dB (phase in rad), b) the same with normalization to 2π rad (periodicity included).

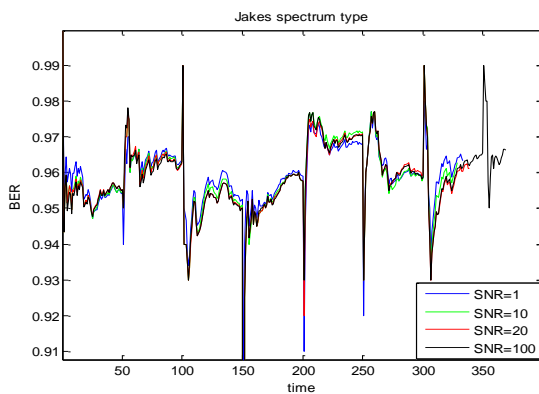


Figure 10. Time dependence of BER for Jakes spectrum type for SNRs 1, 10, 20 and 100 dB for simulated time period.

Fig. 5 shows time change of BER for various SNRs and for the Gaussian spectral type. It can be seen that no significant influence of SNR in communication channel has been exerted on BER over time. Namely, waveforms are similar for different SNRs. BERs are slightly lower for higher SNRs, but it is visible at enlarged figure. For various SNRs, Figures 6, 7, and 8 show the phases of the end-to-end constellation (input/output relationship). Fig. 9 enables an easy view for the comparison of the results from Figures 6, 7, and 8. It can be seen that the lowest SNR produces the largest shift to the right in the figure. However, a waveform remains similar. It means that SNR changes the phase of transmitted signal, which becomes more or less negative. Of course, this can be delusive. If it is considered that only 360° (or 2π rad) can be an angle, and higher values mean more cycles than a totally different figure can obtain. However, if a mean is calculated for input-output variables under various SNRs, central coordinates are obtained. For SNR = 1 dB, mean coordinates are $(-0.0012, -0.0017)$. For SNR = 10 dB, these coordinates are $(-0.0015, -0.0017)$. For SNR = 20 dB, the mean coordinates are $(-0.0012, -0.0017)$.

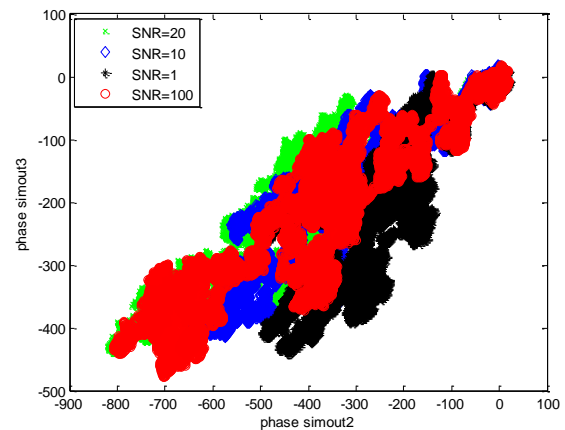


Figure 11. Comparison of phases of the end-to-end constellation in Jakes spectrum type with SNRs 1, 10, 20 and 100 dB (phase in rad).

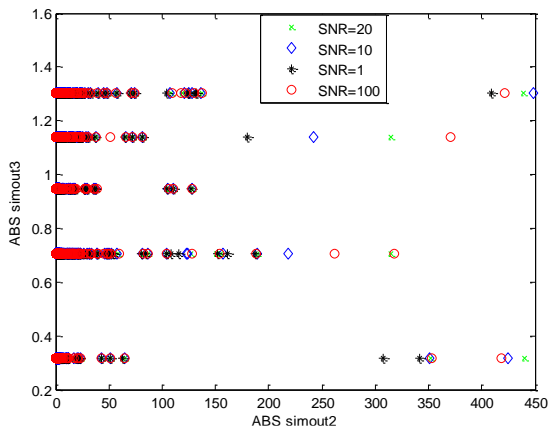


Figure 12. Absolute values (magnitudes of complex signal spectrum) of the end-to-end constellation for Jakes spectrum type with SNRs 1, 10, 20, and 100 dB (all are parameters of the communication channel adjustable in Simulink blocks).

Finally, for SNR = 100 dB, the mean coordinates are $(-5.6597 \times 10^{-4}, -8.8093 \times 10^{-4})$.

These center coordinates can be interpreted as if there are no effects of increased SNR to phase characteristics. But, it can be also noticed that the central point for SNR = 100 dB is (52.8%, 48.18%) closer to the center of the point of origin (0, 0) than the center point for SNR = 1 dB.

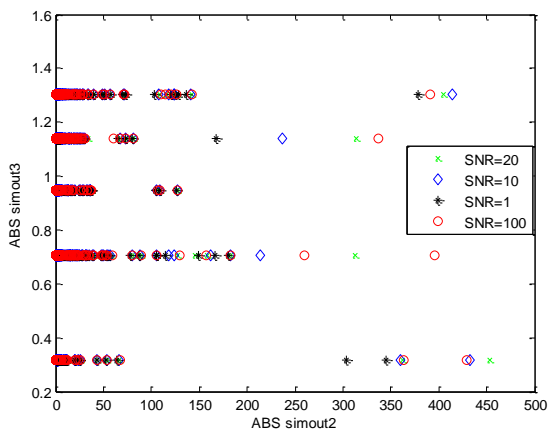


Figure 13. Absolute values (magnitudes of complex signal spectrum) of the end-to-end constellation for Flat spectrum type with SNRs 1, 10, 20, and 100 dB type, parameters adjustable in modeled Simulink blocks (simulation output variables 2 and 3 at different axes).

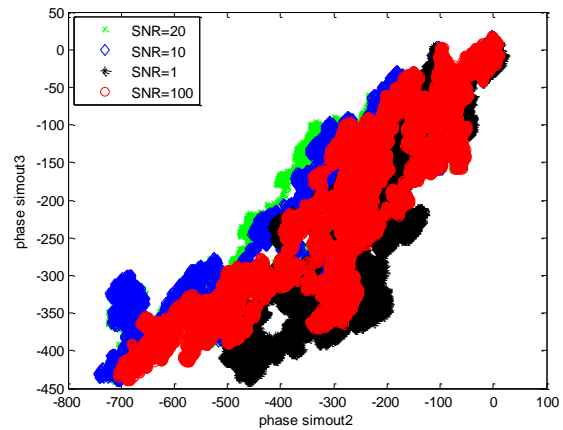


Figure 14. Comparison of phases of the end-to-end constellation in Flat spectrum type with SNRs 1, 10, 20 and 100 dB (phase in rad).

BER time dependence is showed in Fig. 10 for Jakes spectrum type in the simulated time period. Several SNRs were investigated and presented as different curves. It can be seen that the signal exhibits non-stationary oscillations around the average.

Fig. 11 shows comparison of the phases of the end-to-end constellation in the Jakes spectrum type with SNRs 1, 10, 20 and 100 dB. It can be observed that the lowest SNR produces the largest shift to the right.

From Figures 12 and 13, it can be seen that absolute values are not well suited for investigation on spectral types. Different values of SNRs are mixed up and they are hence not suitable for a human observer to reach conclusions. The variable denoted as simout2 is taken between QAM block and raised cosine transmit filter in the transmitter part of the communication system. The variable denoted as simout3 is taken between raised cosine receive filter and QAM block in the receiver part of the communication system. Magnitudes correspond to the dB units, but the point is in the relation between input and output variables. As expected, the magnitudes of the receiver part are significantly lower than from the transmitter part of the communication system.

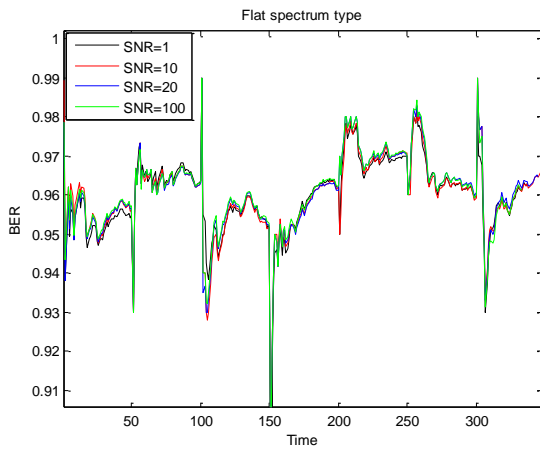


Figure 15. Time dependence of BER for Flat spectrum type for SNRs 1, 10, 20 and 100 dB for simulated time period.

Fig. 14 shows the comparison of the phases of the end-to-end constellation in Flat spectrum type with SNRs 1, 10, 20 and 100 dB. The same conclusions can be also reached in the case of Jakes spectrum type.

Fig. 15 shows time-dependent graph of the BER for the Flat spectrum type for SNRs 1, 10, 20 and 100 dB in the simulated time period. It can be seen that curves for different SNRs are following similar waveforms.

Table 2. presents the influence of the SNR on the mean BER value in the case of the Flat spectrum type. It can be seen that an increase in SNR increases the mean BER value.

Table 2. SNR influence to BER for the Flat spectrum type

SNR [dB]	Mean value of the output signal's BER
1	0.9579
10	0.9601
20	0.9605
100	0.9606

4 Conclusion

This research shows the complexity of ship integrated communication design based on fiber optic media. The paper examines only one problem – the choice of the channel representation and some parameters changes.

It can be concluded that the most reliable spectrum type of the analyzed set is Asymmetrical Jakes. Furthermore, an increase in SNR results in non-proportional and non-significant increase in BER. Furthermore, a phase does not produce useful results for further interpretations.

References

- [1] Kuzmanić, I., Vlašić, R., Vujović, I.: *Materials in electrical engineering*, (in Croatian), Faculty of Maritime Studies, Split, 2001. Presentation of the exact topic available at: http://www.pfst.hr/~ivujovic/stare_stranice/ppt/pred10.ppt (in Croatian).
- [2] Bel Hadj Tahar, J.: *Theoretical and Simulation Approaches for Studying Compensation Strategies of Nonlinear Effects Digital Lightwave Links Using DWDM Technology*, Journal of Computer Science, 3 (2007), 11, pp. 887-893.
- [3] Binh, L. N., Armstrong, J.: *A Simulink Model for Simulation of Optical Communications Systems: Part I – Single-channel Transmission*, Technical Report MECSE-31-2004, Monash University, 2004.
- [4] Binh, L. N.: *MATLAB Simulink Simulation Platform for Photonic Transmission Systems*, International Journal of Communications, Network and System Sciences, 2 (2009), pp. 91-168.
- [5] Xiang, L. S. Chandrasekhar, P. J. W.: *Digital Signal Processing Techniques Enabling Multi-Tb/s Superchannel Transmission*, IEEE Singal Processing Magazine, 31(2014), 2, pp. 16-24.
- [6] Huang, Y.-K., Ip, E., Wang, Z., Huang, M-F., Shao, Y., Wang, T.: *Transmission of spectral efficient super-channels using all-optical OFDM and digital coherent receiver technologies*, Journal of Lightwave Technology, 29 (2011), 24, pp. 3838-3844.
- [7] Zhou, X.: *Efficient Clock and Carrier Recovery Algorithms for Single-Carrier Coherent Optical Systems*, IEEE Singal Processing Magazine, 31 (2014), 2, pp. 35-45.
- [8] Mahros, A. M., Tharwat, M. M.: *Implementation of a Radio-over-fiber OFDM Communication System in the Simulink Environment*, ORACST International Journal of Advanced Computing, Engineering and Application (IJACEA), 1 (2012), 3, 123-128.

- [9] Binh, L. N., Gan, I., Tan, W.: *SIMULINK Model for Optically Amplified Transmission Systems: Part V: Linear and Nonlinear Fiber Propagation Models*, Technical Report MECSE-6-2005, Monash University, 2005.
- [10] Chang, J., Prucnal, P. R.: *A Novel Analog Photonic Method for Broadband Multipath Interference Cancellation*, IEEE Microwave and Wireless Components Letters, 23 (2013), 7, 377-379.
- [11] Cvijetic, M., Djordjevic, I. B.: *Advanced Optical Communication Systems and Networks*, Artech House, Boston, 2013.
- [12] Ivče, R., Jurdana, I., Kos, S.: *Ship's cargo handling system with the optical fiber sensor technology application*, Scientific Journal of Maritime Research, 28 (2014), 118-127.
- [13] Fibre Channel Basics - Fast, affordable, easy-to-configure storage networks, Technology Brief, Apple, available at: https://manuals.info.apple.com/MANUALS/0/MA340/en_US/Fibre_Channel_Basics_TB_v10.4.pdf.
- [14] Shastry, N., Madireddy, U., Ravi, N.: *Simulation of an Optical Fiber Point to Point Communication link using Simulink*, available at: <http://www.ee.eng.buffalo.edu/faculty/paoliu/413/present05/Group11/Group11final.ppt>.
- [15] Kannan, V., Radhakrishnan, R., Palaniyandi, K.: *A review on conventional and laser assisted machining of aluminium based metal matrix composites*, Engineering Review, 34 (2014), 2, pp. 75-84.